Berger Scientfic Press

Innovation & Technology Advances, 2023, 1(2), 47–62
https://bergersci.com/index.php/jta/index
DOI: 10.61187/ita.v1i2.39

Study on flow line characteristics and well test interpretation methods of multi branch fractured wells in dual porous media

Yong Jiang*, Lei Zhang, Haojun Wu, Zhennan Gao, Hua Zheng

Tianjin Branch of CNOOC Limited, Tianjin, China
zhanglei13@cnooc.com.cn (Zhang, L.), wuhj8@cnooc.com.cn (Wu, H.), gaozhn@cnooc.com.cn (Gao, Z.), zhenghua@cnooc.com.cn (Zheng, H.)

*Correspondence: jiangyong6@cnooc.com.cn

Abstract: Fractured reservoirs have developed fractures, strong heterogeneity, and complex seepage patterns. The analysis of core and imaging logging data in Bohai BZ Oilfield shows that there are a large number of fractures developed in the formation, with some wells having up to 6-8 fractures per meter. To study the impact of fractures on seepage, a multi fracture system seepage field simulation method was established, and the characteristic curves of flow lines under different fracture shapes were drawn. The fracture flow line morphology shows that there is a significant difference in the distribution of flow lines between the presence and absence of fractures, and the location of the fractures The size and shape of the reservoir have varying degrees of influence on the distribution of the streamline. The streamline around the well is distributed radially around it. When the fluid encounters an area with developed fractures, it first flows into the fractures and then flows from the fractures towards the wellbore. At the same time, based on the characteristics of fracture development in BZ oilfield and the theory of vertical fracture well testing, a dual medium multi fracture system oil well testing model was established. The model was numerically solved using Laplace transform, and a dual logarithmic curve chart for dual pore medium multi branch fracture well testing was obtained. The effects of fracture branching number, fracture length, conductivity coefficient ratio, and fracture conductivity on the shape of the testing curve were analyzed. The established well testing interpretation model can analyze oilfield stratigraphic information, reservoir fracture development, and boundary conditions. The research results have important guiding significance for evaluating the dynamic performance of oil wells in a dual pore medium multi fracture system and designing oilfield development plans.

Keywords: double porous medium, cracks, streamline, well testing, diversion capacity

How to cite this paper: Jiang, Y., Zhang, L., Wu, H., et al. Study on Flow Line Characteristics and Well Test Interpretation Methods of Multi Branch Fractured Wells in Dual Porous Media. Innovation & Technology Advances, 2023, 1(2), 47–62. https://doi.org/10.61187/ita.v1i2.39

1. Introduction

In recent years, with the increasing exploration and development efforts in Bohai Oilfield, some fractured oil reservoirs have been discovered in deep Archean metamorphic rock buried hills. Currently, these reservoirs have become an important field of oil and gas exploration and development in Bohai. The most important discoveries include the BZ metamorphic rock buried hill fractured oil reservoir, which has oil and gas reserves of up to 100 million tons. Analysis of data such as core and imaging logging shows that the macroscopic fractures in the oil field are developed, and the fracture direction is mainly NEE-SWW direction. The fracture direction is mainly affected by faults, and near areas with large faults and fault system development, the reservoir fractures are developed, and the fracture opening is relatively large. The linear density of fractures in a single well ranges from 4.2 to 8.3 per meter, with a distribution range of fractures 32.2μm~175.7μm. It is a typical fractured oil and gas reservoir with developed fractures. For such reservoirs, fractures not only control the distribution of oil and gas reservoirs, but also serve as the main flow channel for fluids and are important control factors for the

productivity of oil and gas wells. However, due to the complex distribution of fractures and strong heterogeneity of the reservoir, the seepage law becomes more complex.

Sun Qinghe and Zhang Dawei conducted research on well testing analysis methods for evaluating fractured reservoirs and established a finite conductivity vertical fracture bilinear flow model [1,2]. Mou Zhenbao applied the basic method of point source function to establish a coupling model between the reservoir and fractures of vertically fractured wells based on the characteristics of different conductivity at different positions of vertical fractures [3]. Wang Xiaodong studied the complete pressure dynamic characteristics and productivity evaluation method of vertically fractured wells with limited conductivity in closed formations based on the theory of unstable seepage [4]. Li Aifen has completed a new algorithm for solving the finite conductivity vertical fracture well test model in dual porous media [5]. Liu Nengqiang and Zhang Yanyu established a well testing interpretation model for vertically fractured wells in mean oil reservoirs [6,7]. Liu Jianjun obtained a mathematical model for fluid solid coupling seepage calculation in fractured sandstone reservoirs [8]. Cinco proposed bilinear flow model and two-dimensional plane model [9,10]. Lee established a trilinear flow model [11]. Liu Ciqun quickly calculated typical curves for finite conductivity vertical fracture well testing analysis in homogeneous and dual medium reservoirs using the elliptical flow model and mass conservation method [12-15]. Zhang Dezhi established a well testing interpretation model for complex fractured low permeability reservoirs with dual porosity and dual permeability media [16]. However, there is currently limited research on well testing for multi branch fractured wells with multiple fractures. The actual drilling data of Bohai A Oilfield confirms that reservoir fractures are very developed, and these methods have certain limitations in describing the characteristics of formation fluid seepage. This article combines the characteristics of fracture development in Bohai BZ Oilfield to establish a multi fracture system seepage field simulation method and well testing interpretation model, it has important guiding significance for evaluating the dynamic performance of dual medium multi fracture system oil wells and designing oilfield development plans.

2. Simulation analysis of seepage field in multi fracture system

A streamline is a line formed by the tangent lines of the instantaneous flow velocity field of a fluid. The streamline can describe the path of the fluid flowing to the wellbore, and the distribution of the streamline can directly reflect the trajectory of the reservoir fluid movement, helping to determine the impact of fracture distribution on the drainage area and seepage law of multi fracture reservoirs [17-22]. By using streamline, a streamline model can be established to calculate the development performance of oil and gas fields. Therefore, the study of streamline distribution has received widespread attention from reservoir engineering researchers. The distribution of streamline is closely related to the characteristics of the strata and is influenced by many factors. The heterogeneity of oil reservoirs, the presence of impermeable areas, and boundary properties all have varying degrees of impact on the distribution of oil reservoir streamline. If the existence of cracks is determined based on geological data, the location, size, and shape of cracks have varying degrees of impact on the streamline distribution of the oil reservoir. The analysis of core and imaging logging data shows that there are many fractures developed to varying degrees in the Bohai BZ oilfield. To study the impact of fractures on seepage, it is necessary to simulate and analyze the seepage field of the fracture system.

2.1. Establishment of Streamline Simulation Method for Crack System

A typical oil reservoir with a multi fracture system is shown in **Figure 1**. Assuming that the fluid flows stably, the reservoir is homogeneous, isotropic, and of equal thickness, and the fracture development height is consistent with the reservoir height, the control equation is a two-dimensional Laplace equation:

$$\nabla^2 p = 0 \tag{1}$$

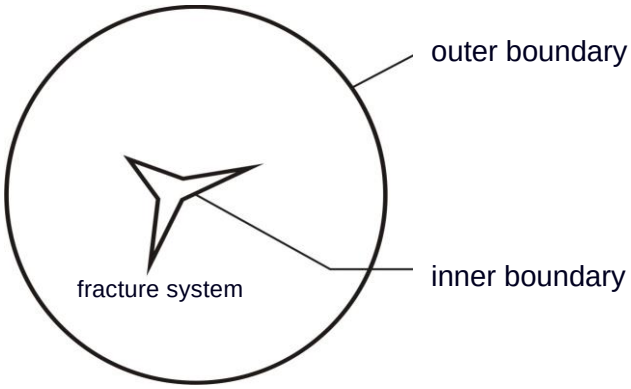

Figure 1. Schematic diagram of multiple fractures in the oil reservoir

The inner boundary is multiple fractures, while the outer boundary is the outer boundary of the reservoir. Equation (1) is a harmonic function in the region, and its fundamental solution is $\frac{1}{2\pi}\ln\frac{1}{r}$. According to Green's formula, the pressure at a point in the region can be associated with boundary conditions:

$$p(M) = \frac{1}{2\pi}\int_s \left[p(S)\frac{\partial \ln r}{\partial n} - \frac{\partial p(S)}{\partial n}\ln r \right] dS \tag{2}$$

$p(M)$ is the pressure at any point, $p(S)$ is the pressure on the boundary.

By discretizing the above equation, the pressure at each point in the entire domain can be obtained from the boundary conditions. In order to perform the closed integral calculation of the boundary integral equation, the constant element method is used for streamline simulation research. The boundary is approximately divided into N straight line segments, and the midpoint of each straight line segment is taken as the node. Generally, it is arranged in order on each boundary element, $p(S)$ and $\frac{\partial p(S)}{\partial n}$ set as constants, their values are respectively equal to the values on the middle node, is $\left[p(S)\right]_j$ and $\left[\frac{\partial p(S)}{\partial n}\right]_j$, Then equation (2) can be discretized as:

$$p(M) = \frac{1}{2\pi}\left[\sum_{j=1}^{N} \left(p(S)\right)_j \int_s \frac{\partial \ln r}{\partial n} dS - \sum_{j=1}^{N} \left(\frac{\partial p(S)}{\partial n} \right)_j \int_s \ln r dS \right] \tag{3}$$

The potential derivative is:

$$\left[\frac{\partial p(M)}{\partial x}\right]_j = \frac{1}{2\pi}\left[\sum_{j=1}^{N} \left(p(S)\right)_j \int_s \frac{\partial}{\partial x}\left(\frac{\partial \ln r}{\partial n}\right) dS - \sum_{j=1}^{N} \left(\frac{\partial p(S)}{\partial n} \right)_j \int_s \frac{\partial (\ln r)}{\partial x} dS \right] \tag{4}$$

$$\left[\frac{\partial p(M)}{\partial y}\right]_j = \frac{1}{2\pi}\left[\sum_{j=1}^{N} \left(p(S)\right)_j \int_s \frac{\partial}{\partial y}\left(\frac{\partial \ln r}{\partial n}\right) dS - \sum_{j=1}^{N} \left(\frac{\partial p(S)}{\partial n} \right)_j \int_s \frac{\partial (\ln r)}{\partial y} dS \right] \tag{5}$$

So the streamline can be obtained based on the following two equations:

$$x_{j+1} = x_j + \frac{k}{\mu}\left[\frac{\partial p(M)}{\partial x}\right]_j dt_j \tag{6}$$

$$y_{j+1} = y_j + \frac{k}{\mu}\left[\frac{\partial p(M)}{\partial y}\right]_j dt_j \tag{7}$$

Given a sufficiently small dt, a streamline can be traced and drawn. In simulation analysis, the inner boundary can be known by potential or derivative; The outer boundary is atmospheric or impermeable. Due to the ease in determining various parameters of cracks at the beginning of the calculation, it is convenient and effective to simulate radial multi crack systems.

2.2 Streamline simulation results

By using Equations (6) and (7), the streamline of the oil reservoir can be plotted. The more nodes there are, the more accurate the results will be; But the time required for calculation also increases accordingly, and as the number of nodes increases to a certain extent, the shape of the line tends to stabilize. From the simulation results (**Figure 2**-**Figure 5**), it can be seen that the streamline distribution map vividly displays the trajectory of fluid movement in fractured formations. The development of fractures has a significant impact on the flow of fluids through the formation. The distribution of flow lines varies greatly between fractures and non fractures, and the location, size, and shape of fractures have varying degrees of influence on the distribution of flow lines in oil reservoirs. The flow line around the well is distributed radially around it. When the fluid encounters an area with developed fractures, it first flows into the fractures and then flows towards the wellbore from the fractures.

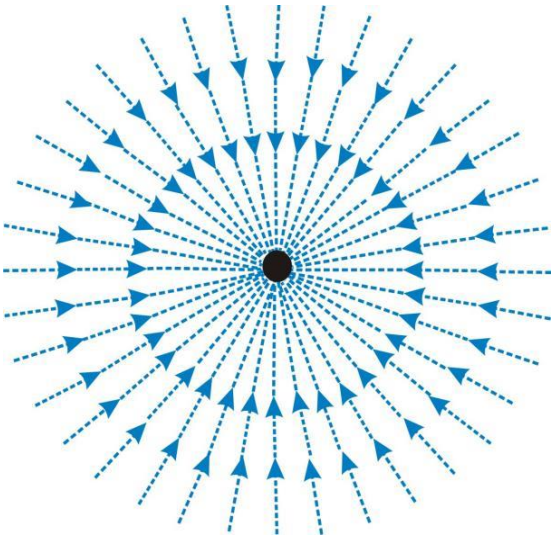

Figure 2. Streamline distribution without cracks

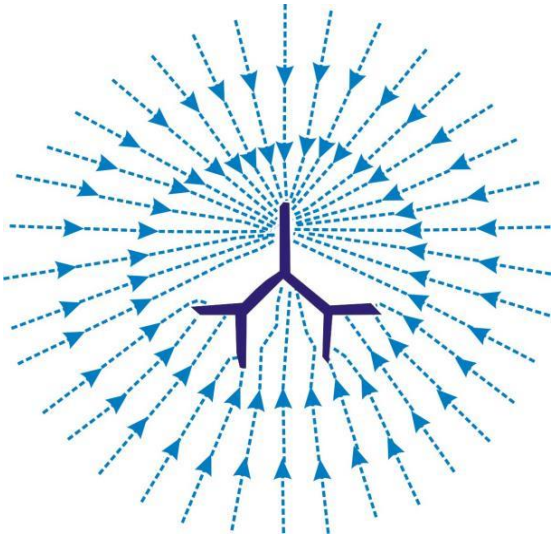

Figure 3. Distribution of Three Branch Cracks and Streamlines

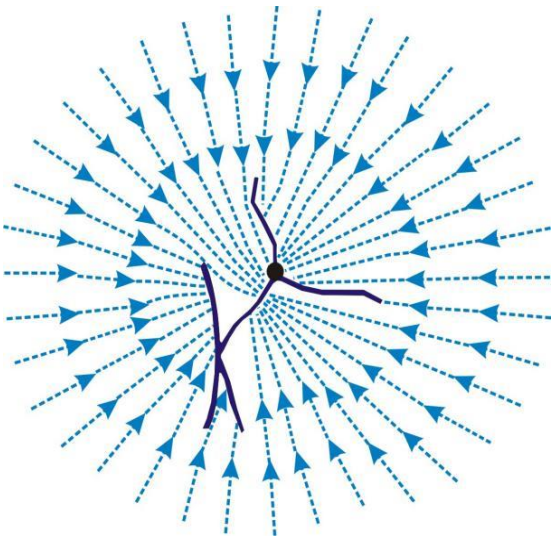

Figure 4. Distribution of tortuous cracks and streamline

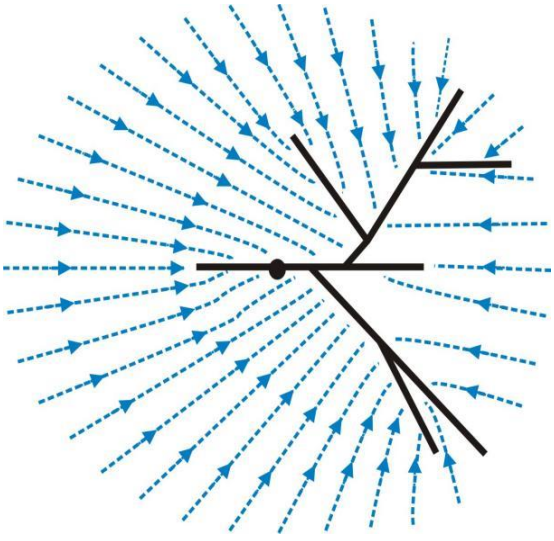

Figure 5. Distribution of multi branched cracks and streamline

3. Well testing modeling methodology

3.1 Establishment of mathematical models

Due to the irregular and complex distribution of fractures in the actual dual medium formations of oil fields, there are considerable difficulties in studying the flow patterns of fluids through them. In order to study the flow patterns of fluids in dual media, a simplified Warren Root physical model was used (**Figure 6**). Consider a dual medium reservoir as two systems: a fracture system and a matrix rock block system, and these two systems exist within any volume unit in the reservoir. Assuming that the permeability of the fracture system K_f is much higher than that of the matrix rock block system K_m, $K_f >> K_m$; And crude oil flows from the matrix rock block to the fracture system, and then from the fracture system to the wellbore.

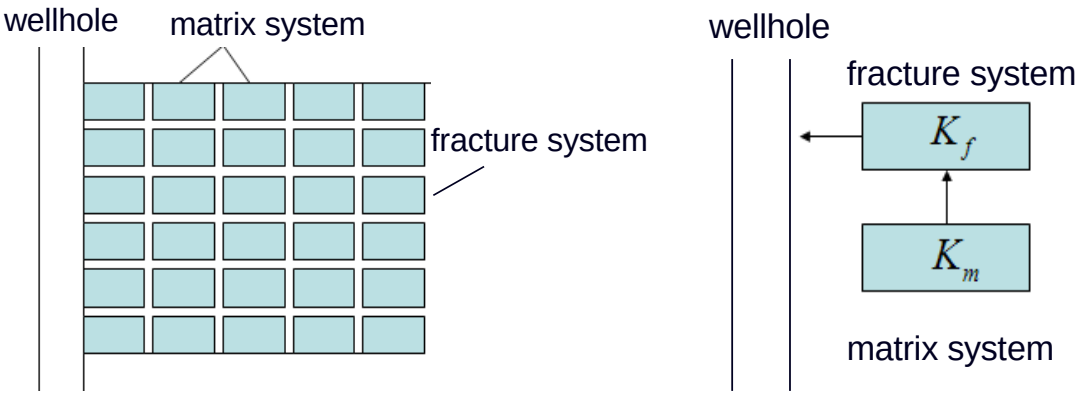

Figure 6. Dual porosity medium reservoir model.

Based on this, combined with the development of fractures in Oilfield A, the following basic assumptions are made for the oil reservoir:

1) Assuming that there is a well in the center of a circular constant pressure boundary double hole formation for constant production rate, and n finite conductivity fractures of length x_f and width ω_f are developed radially around the well. The fractures are symmetrically developed, and the formation replenishes fluid to the wellbore through the fractures. The physical model is shown in **Figure 7**.

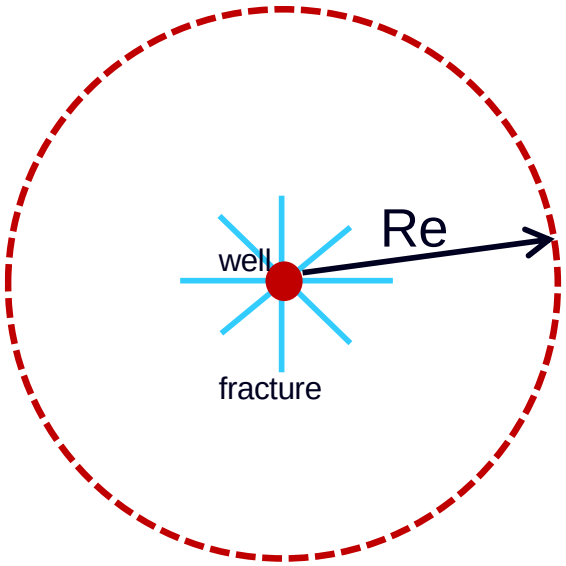

Figure 7. Physical model of multi branch vertical fractured wells

2) The fractures and formation fluids are slightly compressible, and the compressibility coefficient remains unchanged;

3) Neglecting the influence of gravity and capillary force;

4) The fracture conductivity does not vary with location and is a finite constant;

5) Both the strata and fractures are single-phase flow and comply with Darcy's law;

6) Consider wellbore storage and crack skin effects.

Under the above assumptions, establish a differential equation describing the seepage of fractures and formations.

The equation of fracture:

$$\frac{\partial^2 p_f}{\partial r^2}+\frac{2k}{k_f\omega_f}\frac{\partial p}{\partial n}=\frac{\partial p_f}{\partial t}\frac{\mu\phi_f C_f}{k_f} \tag{8}$$

Formation equation: 1 represents the formation fracture system, 2 represents the formation matrix system.

Formation fracture system:

$$\frac{k_1}{\mu}[\frac{1}{r}\frac{\partial}{\partial r}(r\frac{\partial p_1}{\partial r})+\frac{1}{r^2}\frac{\partial^2 p_1}{\partial\theta^2}]+\lambda\frac{k_2}{\mu}(p_2-p_1)=\phi_1 C_{t,1}\frac{\partial p_1}{\partial t} \tag{9}$$

Formation matrix system:

$$\lambda\frac{k_2}{\mu}(p_2-p_1)=\phi_2 C_{t,2}\frac{\partial p_2}{\partial t} \tag{10}$$

Inner boundary conditions:

Wellbore storage effect:

$$(n\frac{k_f\omega_f h}{\mu}\frac{\partial p_f}{\partial r})\Big|_{r_w}=Bq+C\frac{dp_w}{dt} \tag{11}$$

Skin effect:

$$(p-p_f)\Big|_{\Gamma_f}=\frac{Sx_f}{2\pi}\frac{\partial p}{\partial n} \tag{12}$$

Outer boundary conditions:

Fracture:

$$\frac{\partial p_f}{\partial r}\Big|_{x_f}=0 \tag{13}$$

Constant pressure outer boundary:

$$p\Big|_{r_e}=p_i \tag{14}$$

Initial condition:

Stratum:

$$p\Big|_{r_e}=p_i \tag{15}$$

Fracture:

$$p\big|_{r_e} = p_i \tag{16}$$

Dimensionalize the above model and take Laplace transform, the results are as follows:

The equation of fracture:

$$\frac{\partial^2 \overline{p}_{fD}}{\partial r_D^2} + \frac{2}{L_{fD}} \frac{\partial \overline{p}_D}{\partial n_D} = z\eta \overline{p}_{fD} \tag{17}$$

The equation of formation:

$$\frac{1}{r}\frac{\partial}{\partial r}(r\frac{\partial \overline{p}_D}{\partial r}) + \frac{1}{r^2}\frac{\partial^2 \overline{p}_D}{\partial \theta^2} = z\frac{\lambda + z\omega(1-\omega)}{\lambda + z(1-\omega)}\overline{p}_D \tag{18}$$

Inner boundary conditions:

Wellbore storage effect:

$$(\frac{nL_{fD}}{2\pi}\frac{\partial \overline{p}_{fD}}{\partial r_D})\Big|_{\frac{r_w}{x_f}} = C_D z \overline{p}_{wD} - \frac{1}{z} \tag{19}$$

Skin effect:

$$(\overline{p}_D - \overline{p}_{fD})\big|_{\Gamma_f} = \frac{2S}{\pi}\frac{\partial \overline{p}_D}{\partial n_D} \tag{20}$$

Outer boundary conditions:

Fracture:

$$\frac{\partial \overline{p}_{fD}}{\partial r_D}\Big|_{r_D=1} = 0 \tag{21}$$

Constant pressure outer boundary:

$$\overline{p}_D\Big|_{r_D=\frac{r_e}{x_f}} = 0 \tag{22}$$

Where the dimensionless Laplace space pressure is $\overline{p}_D = \int_0^\infty p_D(r_D, t_D)e^{-zt_D}dt_D$;

The dimensionless pressure is $p_D = \frac{p_i - p}{p_i - p_{wf}}$;

The dimensionless distance is $r_D = \frac{r}{x_f}$;

The dimensionless time is: $t_D = \frac{kt}{\mu\phi C_t x_f^2}$;

The dimensionless conductivity is $L_{fD} = \frac{k_f \omega_f}{k x_f}$;

The ratio of conductivity coefficient between fracture and matrix is $\eta = \frac{k\phi_f C_f}{k_f \phi C_t}$;

The dimensionless well storage coefficient is $C_D = \frac{C}{2\pi h\phi C_t x_f^2}$

Parameter Description: Z is Laplace space variable; B is the volume coefficient of the fluid , dimensionless; S is skin coefficient, dimensionless; C is well storage coefficient, m^3/MPa; C_f is the comprehensive compressibility of fluid in fracture, 1/MPa; C_t is the comprehensive compressibility of fluid in formation, 1/MPa; h is the formation thickness, m; K is the permeability of formation, μm^2; K_f is the permeability of fracture, μm^2; ω is storativity ratio, dimensionless; λ is the interporosity flow parameter, dimensionless; x_f is the half-lenth of fracture, m; ω_f is the fracture width, m; q is the production, m^3/d; μ is the fluid viscosity, mPa•s; Φ is the total porosity, dimensionless; Φ_f is the porosity of fracture, dimensionless; P is the pressure in the formation, MPa; P_i is the initial pressure, MPa.

3.2 Mathematical Model Solving

It can be used to solve the model of the implicit difference scheme method [23,24]. The radial direction exponential grid is divided into N grids, $\Delta x = \frac{1}{N}\ln(\frac{r_e / x_f}{r_w / x_f}) = \frac{1}{N}\ln(\frac{r_e}{r_w})$, $r_i = \frac{r_w}{x_f}e^{(i+0.5)\Delta x}$, considering the symmetrical distribution of fractures, the area where two adjacent fractures and the angle are located is taken as one unit for research. Divide the angle into M grids according to a uniform grid, $\Delta\theta = \frac{2\pi}{n\times M}$; it is divided into $N\times M$ grids. Each grid equation:

$$aw_{i,j}p_{i-1,j} + ae_{i,j}p_{i+1,j} - \left(ac_{i,j} + z\frac{\lambda + z\omega(1-\omega)}{\lambda + z(1-\omega)}\right)p_{i,j} + an_{i,j}p_{i,j-1} + as_{i,j}p_{i,j+1} = 0 \tag{23}$$

Where:

$$aw_{i,j} = ae_{i,j} = \frac{1}{r_i^2\Delta x^2} \tag{24}$$

$$an_{i,j} = as_{i,j} = \frac{1}{r_i^4\Delta\theta^2} \tag{25}$$

$$ac_{i,j} = aw_{i,j} + ae_{i,j} + an_{i,j} + as_{i,j} \tag{26}$$

Fracture is divided into $L\times 2$ grids. Each grid equation:

$$aw_{i,j}p_{i-1,j} + ae_{i,j}p_{i+1,j} - (ac_{i,j} + z\eta)p_{i,j} + an_{i,j}p_{i,j-1} + as_{i,j}p_{i,j+1} = ar_{i,j} \tag{27}$$

Where:

$$aw_{i,j} = ae_{i,j} = \frac{1}{r_i^2\Delta x^2} \tag{28}$$

$$an_{i,j} = \frac{2}{L_f[r_i\frac{\Delta\theta}{2}(1+\frac{S\Delta x}{\pi\Delta\theta})]},\ as_{i,j} = 0 \tag{29}$$

$$as_{i,j} = \frac{2}{L_f[r_i \frac{\Delta\theta}{2}(1+\frac{S\Delta x}{\pi\Delta\theta})]}, an_{i,j} = 0 \tag{30}$$

$$ac_{i,j} = aw_{i,j} + ae_{i,j} + an_{i,j} + as_{i,j} \ \nabla^2 p = 0 \tag{31}$$

Correction of grid connection in fractured wellbore:

$$ac_{1,1} \Leftarrow ac_{1,1} - \frac{C_D z}{\frac{2C_D z\pi \frac{r_w}{x_f}\Delta x}{L_f} + 2n} \tag{32}$$

$$ar_{1,1} \Leftarrow ar_{1,1} - \frac{\frac{1}{z}}{\frac{2C_D z\pi \frac{r_w}{x_f}\Delta x}{L_f} + 2n} \tag{33}$$

$$aw_{1,1} = 0, ae_{L,1} = 0 \tag{34}$$

Calculation formula for wellbore pressure:

$$p_w = \frac{\frac{1}{z} + \frac{L_f \cdot n}{\pi \frac{r_w}{x_f}\Delta x} p_1}{C_D z + \frac{L_f \cdot n}{\pi \frac{r_w}{x_f}\Delta x}} \tag{35}$$

The bottom hole pressure calculated above is the solution in Laplace space, with the help of Stehfest Laplace numerical inversion transformation algorithm [25], obtain dimensionless bottom hole pressure in real space p_{wD}, the basic formula of Stehfest Laplace numerical inversion transformation algorithm is as follows:

$$p_D(t) = \frac{\ln 2}{t}\sum_{i=1}^{N} v_i \overline{p_D}(z_i) \tag{36}$$

$$z_i = (\ln\frac{2}{t}) \cdot i \tag{37}$$

$$v_i = (-1)^{i+N/2} \sum_{k=(i+1)/2}^{\min(N/2,i)} \frac{k^{N/2}(2k)!}{(N/2-k)!(k!)(k-1)!(i-k)!(2k-i)!} \tag{38}$$

3.3 Type curves and sensitivity analysis

3.3.1 Effect of fracture branch number on the characteristics of well testing curve

By solving the model, the dynamic response curve of multi-branch fracture well pressure in dual-porosity reservoir can be obtained. **Figure 8** reflects the influence of fracture branch number on the dynamic curve of bottom hole pressure. From the double logarithmic curve in the figure, it can be seen that the pressure curve is roughly divided into four flow stages: early linear flow stage, elliptic flow stage, channeling flow stage and late radial flow stage. With the increase of the number of fracture branches, the fracture linear flow section is more obvious, while the bilinear flow section is difficult to observe, but the elliptic flow section also appears earlier. This is because the more the fracture branches, the larger the contact surface between the fracture and the formation, and the greater the fracture conductivity.

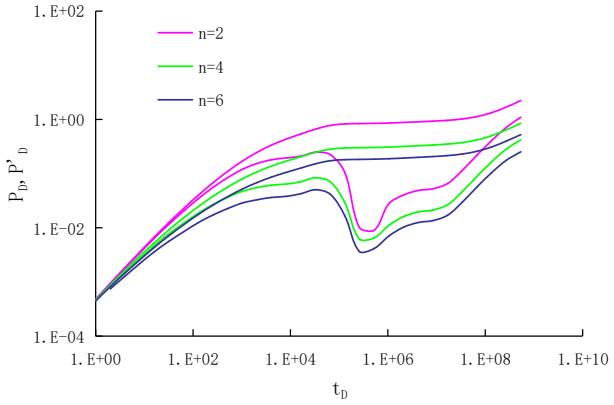

Figure 8. Effect of fracture branch number on double logarithmic curve.

3.3.2 Effect of fracture half-length on the characteristics of well testing curve

The influence of different fracture half-length on the characteristics of well test curve is shown in **Figure 9**. From the double logarithmic curve in the figure, it can be seen that the influence of fracture half-length on the two stages of linear flow and elliptical flow is obvious. The larger the fracture half-length, the more obvious the fracture linear flow section and the longer the duration, while the bilinear flow section is more obvious, and the elliptical flow section appears later. This is because the greater the fracture half-length, the greater the contact surface between the fracture and the formation, the more fluid is added to the fracture by the formation, and the greater the fracture conductivity.

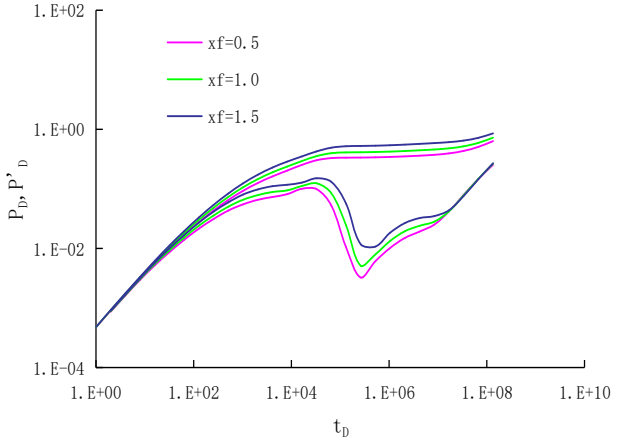

Figure 9. Effect of fracture half-length on double logarithmic curve.

3.3.3 Effect of pressure conductivity coefficient ratio on the characteristics of well testing curve

Figure 10 reflects the influence of pressure conductivity coefficient ratio on the dynamic curve of the bottom hole pressure. It can be seen from the double logarithmic curve in the figure that the larger the ratio of the conductivity coefficient is, the more obvious the linear flow section of the fracture is, and the bilinear flow section is more difficult to observe. The later the elliptical flow section appears. This is because the larger the fracture conductivity ratio, the greater the difference between the fracture and the formation physical properties, and the greater the dominant role of the fracture.

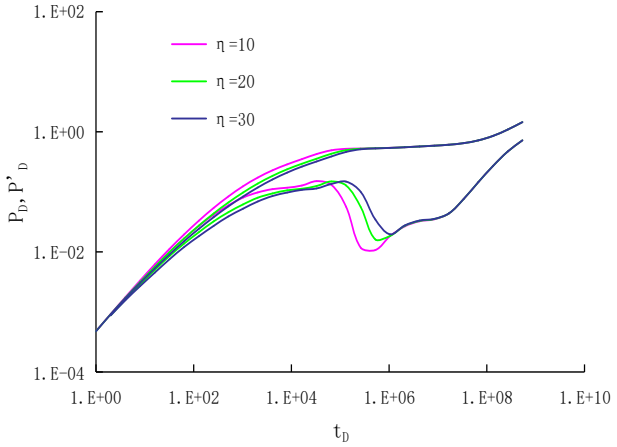

Figure 10. Effect of pressure conductivity coefficient ratio on double logarithmic curve.

3.3.4 Effect of fracture conductivity on the characteristics of well testing curve

Fracture conductivity is one of the most important parameters of fractured reservoir, which is the main embodiment of fracture permeability and fracture width. **Figure 11** reflects the influence of different fracture conductivity on the characteristics of well test curve. It can be seen from the double logarithmic curve in the figure that the larger the fracture conductivity is, the more obvious the linear flow section of the fracture is, and the later the elliptical flow section appears. Because the greater the fracture conductivity, the stronger the fracture communication ability, the more obvious the fracture linear flow.

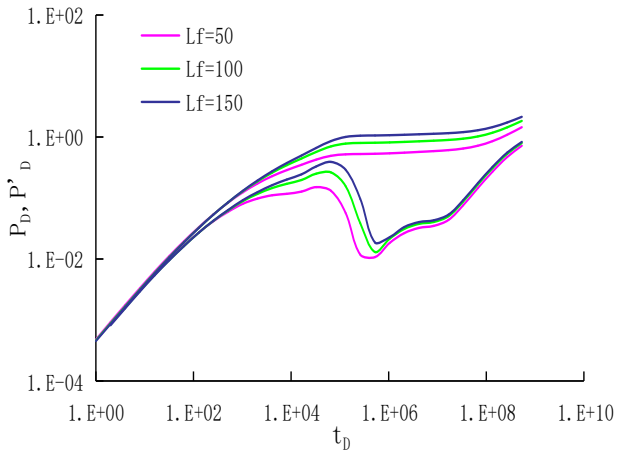

Figure 11. Effect of fracture conductivity on double logarithmic curve.

3.3.5 Effect of cross flow coefficient on type curve

The channeling coefficient represents the ratio of bedrock permeability to fracture permeability and a function of the geometric structure of the matrix rock block. Its numerical value reflects the difficulty of crude oil flowing from the matrix rock block system to the fracture system, and determines the time when the transition period occurs. **Figure 12** reflects the influence of the cross flow coefficient on the well testing curve. As the cross flow coefficient continues to increase, the concave part of the pressure derivative transition section appears earlier and earlier, indicating that the fluid supply capacity of the bedrock to the fracture is becoming stronger. On the contrary, the smaller the channeling coefficient, the later the pressure derivative curve appears, indicating that a larger pressure difference and a longer time are required for the bedrock to supply fluid to the fracture.

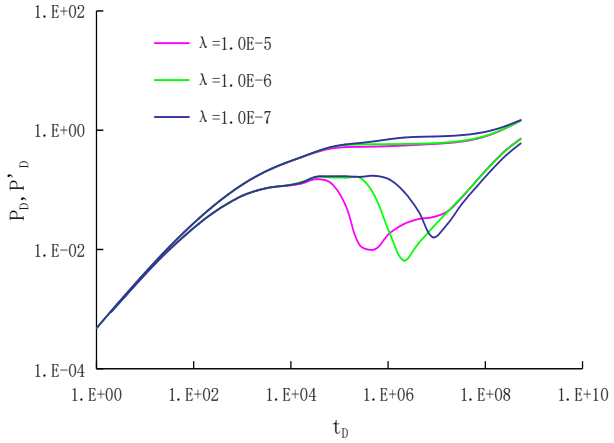

Figure 12. Effect of cross flow coefficient on type curve.

3.3.6 Effect of storativity ratio on type curve

The elastic energy storage ratio represents the ratio of the elastic reserves of crude oil in a fractured system to the total elastic reserves of the system. **Figure 13** reflects the influence of the elastic energy storage ratio on the well testing curve. The elastic energy storage coefficient affects the degree of depression in the pressure derivative curve. As the elastic energy storage ratio decreases, the pressure derivative curve becomes deeper and the starting position of the transition section moves forward, indicating that the supply of bedrock to the fracture has an increased impact on pressure changes.

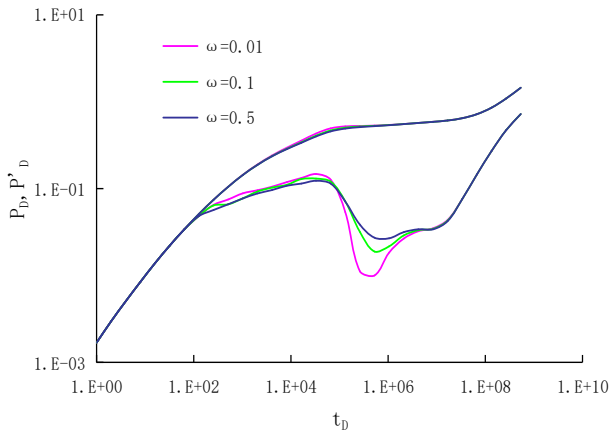

Figure 13. Effect of storativity ratio on type curve.

4. Field Tests Interpretation

The target layer of Bohai BZ Oilfield is the Archaean buried hill. Analysis of core and imaging logging data shows that the reservoir fractures in this block are developed. DST testing was conducted on the exploration well BZ-1, and the relevant basic data of this well are shown in **Table 1**.

Table 1. Basic parameters of reservoir and well.

Parameter	Numerical Value
Oil layer thickness, h (m)	87.3
oil volume factor, B (m^3/m^3)	2.637
well radius, r_w (m)	0.108
Formation crude oil viscosity, μ (mPa·s)	0.27
Formation compressibility coefficient, C_t (1/MPa)	0.00065
Porosity, Φ (%)	4.6
Test production capacity, Q (m^3/d)	312
Test time, t/(h)	212

The established model was used to analyze the DST test data during the testing time. The fitting between the measured pressure data and the typical chart is shown in **Figure 14**. It can be seen that the fitting results of the interpreted chart are in good agreement with the on-site test data. The example explanation parameters are shown in **Table 2**. From the fitting results, it can be seen that the reservoir around BZ-1 well has developed fractures and good physical properties, and there is a certain degree of pollution in the oil well. Based on the comprehensive analysis and understanding of well testing data, it has a foundation for high and stable production. Based on the understanding of well test interpretation results, this block has implemented four trial production wells in the early stage, with a daily oil production of 260-356m^3/d, it has been in operation for 3 years, with stable production and good development results.

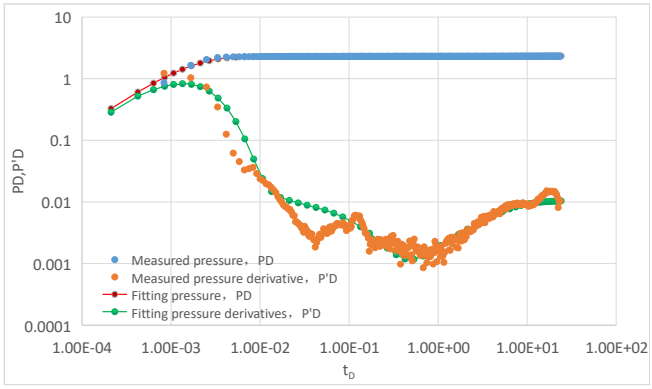

Figure 14. Double logarithmic curve fitting diagram of BZ-1 well.

Table 2. Well test interpretation results.

Parameter	Numerical Value
Permeability, K (mD)	97.6
Skin factor, S	23.9
Number of crack branches, n	5
Half-length of crack, x_f (m)	156.8
Well storage coefficient, C (m^3/MPa)	0.0012
Interporosity flow coefficient, λ	2.65×10^{-7}
Elastic energy storage ratio, ω	0.04
Detecting radius, r (m)	956

5. Conclusions

1) The seepage field simulation method of multi-fracture system is established, and the streamline characteristic curves under different fracture shapes are drawn. The location, size and shape of the fracture have different effects on the streamline distribution of the reservoir. The streamline around the well is radially distributed. When the fluid encounters the area with fracture development, the fluid first flows into the fracture, and then flows from the fracture to the wellbore.

2) Based on the theoretical model of fractured reservoir, combined with the fracture development of BZ oilfield, the well test interpretation model of dual medium multi-fracture system reservoir is established. The model is numerically solved by Laplace transform, and the double logarithmic curve chart of multi-branch fracture well test in dual porosity medium is obtained. The effects of fracture branch number, fracture length, conductivity coefficient ratio and fracture conductivity on the double logarithmic curve are studied.

3) The established well test interpretation model comprehensively considers the fracture characteristic parameters, the flow of the fracture system, and the channeling between the fracture system and the matrix system. According to the well test data, the oilfield formation information, reservoir fracture development and boundary conditions can be analyzed. It has been applied to the interpretation of well test data of fractured reservoirs in Bohai BZ oilfield to guide the design of well location, and has achieved good application results. The research results have important guiding significance for evaluating the dynamic of oil wells in dual-medium multi-fracture system and the design of oilfield development plan.

References

1. Sun, Q. Well testing analysis for evaluating fractured reservoirs. Beijing, China Petroleum Industry Press, 1995.
2. Zhang, D., Zeng, Z. Application of bilinear flow model for finite conductivity vertical fractures. Special Oil & Gas Reservoirs, 2007, 14(4), 72-74.
3. Mou, Z., Fan, Tai. Mathematical model with un-steady-state filtering flow of vertically fractured well with varying conductivity for closed cirlcle oil reservoir. Petroleum Geology and Recovery Efficiency, 2006, 13(6), 66-69.
4. Wang, X., Zhang, Y., Liiu, C. Productivity evaluation and conductivity optimization for vertically fractured wells. Petroleum Exploration and Development, 2004, 31(6), 78-81.
5. Li, A., Liu, Z., Yang, Y. New approach to welltest interpretation model with finite conductivity vertical fracture in double porosity reservoirs. Chinese Journal of Hydrodynamics, 2006, 21(2), 217-222.
6. Liu, N. Practical modern well testing interpretation methods. Beijing, China University of Petroleum Press, 2003.
7. Zhang, Y., Yao, J. Principles and methods of modern well testing interpretation. Beijing, China University of Petroleum Press, 2003.
8. Liu, J., Du, G. An equivalent model of fluid-solid coupling flow in fractured sandstone reservoir. China Offshore Oil and Gas (Geology), 2002, 17(3), 204-210.
9. Cinco L. H., Samaniego V. F., Dominguez A. N. Transient pressure behavior for a well with a finite-conductivity vertical fracture. Society of Petroleum Engineers Journal, 1978, 18(04), 253-264. https://doi.org/10.2118/6014-PA
10. Guppy, K. H., Kumar, S., Kagawan, V. D. Pressure-transient analysis for fractured wells producing at constant pressure. SPE Formation Evaluation, 1988, 3(1), 169-178. https://doi.org/10.2118/13629-PA
11. Azari, M., Wooden, W. O., Coble, L. E. A new approximate analytic solution for finite conductivity vertical fractures. Society of Petroleum Engineers Formation Evaluation, 1986, 18 (2),75-88. https://doi.org/10.2118/20556-MS
12. Liu, C. Transient pressure behavior of a well with a vertical fracture with finite-conductivity in a reservoir with double-porosity. Acta Petrolei Sinica, 1990, 11(4), 61-67.
13. Liu, C. Flow dynamics of vertically fractured wells. Well Testing, 1990, 1(4), 1-4.
14. Liu, Y., Liu, C. A quick well test method of well with infinite conductivity vertical fracture. Petroleum Geology & Oilfield Development in Daqing, 1993, 12(4), 55-60.
15. Liu, C. Well testing analysis method for finite flow vertical fractured wells considering wellbore storage and skin effects. Well Testing, 1993, 5(2), 20-21.
16. Zhang, D. The theory and method of well test interpretation for complex fractured low permeable reservoirs. Beijing, University of Petroleum (Beijing), 2006.

17. Numbere, D. T, Tiab, D. An improved streamline-generating technique that uses the boundary (integral) element method. SPERE, 1988, 3(3), 1061-1068.
18. Sato, K, Horne, R. N. Perturbation boundary element method for heterogeneous reservoirs: Part 1-steady-state flow problems. SPE Formation Evaluation, 1993, 8(4), 315-322. https://doi.org/10.2118/25299-PA
19. He, Y., Yin, H., Liu, L., et al. Research on streamline distribution of flow through heterogeneous porous media with complex boundary. Chinese Journal of Computational Mechanics, 2007, 24(5), 708-712.
20. Xu, X., Yang Z., Zu, L., et al. Equivalent continuous medium model and numerical simulation of multimedia reservoir. Fault Block Oil & Gas Field, 2010, 17(6), 733-737.
21. He, Y., Yin, H. Research on streamline distribution of flow through anisotropic porous media with complex boundary. Xinjiang Petroleum Geology, 2006, 27(2), 204-206.
22. Xu, L., Yin, H. Effect of impermeable area on distribution of flow path in seepage flow field. Petroleum Geology & Oilfield Development in Daqing, 2006, 25(4), 57-59.
23. Chen, Y. Fundamentals of reservoir numerical simulation. Beijing, China University of Petroleum Press, 2006.
24. Lu, J., Guan, Zhi. Numerical methods for partial differential equations. Beijing, Tsinghua University Press, 2006.
25. Jia, Y., Zhao B. Application of Laplace transform and numerical inversion to welltest analysis. Natural Gas Industry, 1992, 12(1), 60-64.